Electronic Supplementary Material (ESI) for Physical Chemistry Chemical Physics.

Supporting Information

Carbon encapsulated nanoscale iron/iron-carbide/graphite particles for EMI shielding and microwave absorption

Rajeev Kumar[*, a], *Harish Kumar Choudhary*[*, a], *Shital Patangrao Pawar*[*, b], *Suryasarathi Bose*[b] *and Balaram Sahoo*[†, a]

Contents

1. Selection of the sample composition

It is well known that density of carbonyl iron (CI) and Electrolytic iron (EI) is higher (7.846 g/cc) than that of the PVDF (1.7 g/cc) or carbonaceous materials. For same volume fraction, the weight of the composites with CI or EI will be very heavy in comparison to the FeC based specimens. High wt% of the metallic phase will no longer make the composite practical to prepare a light-weight EMI shield. In composites having high wt% of the metallic phase, the reflection of EM wave from the surface of the specimen will lead to quite high SE_T, but it will result in EM pollution due to the reflected waves. Furthermore, with increase in concentration of the microwave absorbing particles (filler) the SE_T value increases. But, above a certain concentration of filler, the composite becomes heavy, brittle and non-practical to work with. Thus, we chose a 50:50 wt% to ensure a healthy compromise between the above factors. At this weight ratio (50:50), our composite are light-weight and mechanically tough, which can be directly utilized in designing the EM shield at industrial level. However, choosing the particular (50:50 wt%) composition of the PVDF-FeC is somewhat arbitrary but is used as a standard for comparing the SE_T of all our samples.

2. Sample composition: weight% versus volume%

The aim of the present work is to prepare light weight and low-cost composites with PVDF matrix for efficient EMI shielding applications. Along with volume or weight percent, the size of and homogenous dispersion of the particles play important roles in determining the efficiency of microwave absorption and shielding. This is one of the important results of this work. Although weight percent can always be expressed in terms of volume percent, it is always erroneous to express volume percent of *porous materials*. However, for a better comparison with other reports, the composition of our samples is converted to vol% and is listed in *Table S1* of the supporting information file.

The primary reason for expressing the composition in wt% instead of vol% is the following. It is difficult to calculate the vol% of our prepared carbon@iron/iron-carbide@graphite due to the porosity of the sample and the amorphousness of the carbon matrix. Hence, these porous samples, when compressed to form the toroidal specimens for EMI measurement, the vol%

cannot be an accurate measure. Density of porous samples can vary with the compactness or applied pressure, leading to an error in the measured vol%.

Table S1: Comparison in SE_T versus thickness, sample composition and sample weight among different PVDF based composites reported in the literature and in the present work.

Material	**Equivalent Vol%**	**Equivalent Wt%[#]**	**SE_T (dB)**	**Frequency (GHz)**	**Thickness (mm)**	**Wt(1cc) (g)**	**Ref.**
PVDF-70 vol % graphite	70	74	55-57	8.2-18	1	1.97	[1]
PVDF-70 vol % graphite	70	74	73	8.2-18	1.5	1.97	[1]
PVDF-70 vol % graphite	70	74	90	8.2-18	2	1.97	[1]
PVDF-30 vol % nano Ag	30	72.6	45	8.2-18	1	4.34	[1]
PVDF-70 vol % graphite stacked with PVDF-30 vol % nano Ag	-	73.3[*]	94	8.2-18	1	3.15	[1]
PVDF-25 vol% Cu nanoparticles	25	62.5[a]	120	3.06×10^{-3}		3.52	[2]
PVDF/PS/HDPE-1.6 vol% MWCNT composite	1.6	-	25-31	8-12	2.5	1.70	[3]
PVDF-35 vol% 16 nm Fe metal powder	35	71[b]	40	12	1.95	3.85	[4]
PVDF-20 vol% nano BaTiO3-10 vol% Ag composite	-	69	26	10	1.2	3.44	[5]
PVDF-50 vol% carbonyl iron composites	50	82	20-23	8-12.4	1.2	4.77	[6]
PVDF and multiwall carbon nanotubes (15 wt% MWCNTs)	-	15	50-70	8-12	2	1.75	[7]
PVDF/FeC (50:50 wt% composites)	48.6	50	10-24	8-18	5	1.7	Present work
PVDF/EI (50:50 wt% composites)	17.8	50	9-17	8-18	5	2.78	Present work
PVDF/CI (50:50 wt% composites)	17.8	50	7-9	8-18	5	2.78	Present work
PVDF/a-C (50:50 wt% composites)	53	50	1-2	8-18	5	1.59	Present work

Note: [#]calculated using standard values of density of the material. Please note these values are inferred and are not mentioned in the reference article. Wt(1cc) = the weight of 1 cc of the composite in g.[*] average of two layers, [a] mentioned in literature, [b]

assuming 10 mm x 25 mm sample. The densities taken for the above calculations are as below: PVDF (1.7 g/cm³), Graphite (2.09 g/cm³), Ag (10.5 g/cm³), Fe (7.846 g/cm³), $BaTiO_3$(6.02 g/cm³), amorphous carbon (1.5 g/cm³), Fe_3C (7.05 g/cm³). From the table, it is worth knowing that the equivalent loading of the particle (weight%) in polymer matrix is higher than our prepared PVDF/FeC composite. PVDF/CI and PVDF/EI (Fe metal in PVDF matrix) composite has 17.8 vol% which corresponds to 50 wt% particle loading. Hence, our synthesized FeC particles has higher volume fraction for same loading in wt% which is helpful in designing lightweight and effective EMI shield.

Although the volume percent of EI and CI based samples can be calculated exactly (as these particles do not contain pores in the specimen), the comparison with carbon@iron/iron-carbide@graphite based specimen will not be reasonable. Secondly, as our aim was to demonstrate the effect of encapsulation and size of the magnetic particles on EMI shielding, rather than obtaining an excellent metallic shield (as higher metallic vol% will show high SE_T), we have adopted to express the amount of material accurately in terms of wt%. Thirdly, it is much more convenient to weigh the sample while preparing the specimens than considering the volume fraction.

3. Reitveld refinement of XRD patterns of FeC, CI and EI powder.

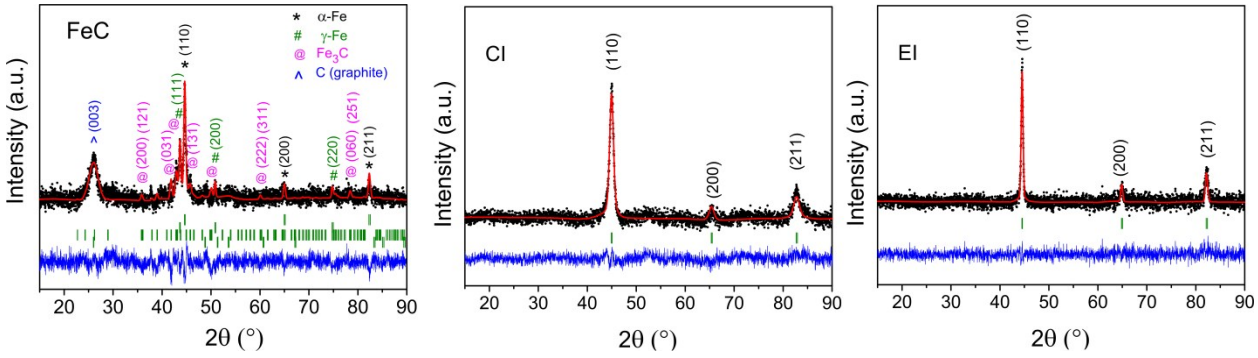

Figure S1. Reitveld refined XRD patterns of FeC, CI and EI. The black dots represent the data points and red line is the fitted Reitveld refined x-ray intensity. The Braggs position of all the phases where indexed as olive colored vertical lines. The blue line at the bottom represents the difference between the calculated and measured intensity.

Fig. S1 shows the Reitveld refinement of the powder XRD pattern of FeC, CI and EI powder samples. "FULLPROF" computer program was used for the refinement. The phases present in the samples were identified using ICSD database and fitted with Reitveld refinement method.

From the refined XRD pattern the lattice parameters, cell volume and average crystallite size were estimated as listed in Table S1. The results for the FeC sample are discussed in the main paper.

Table S2. Structural parameters obtained from the Rietveld refinement of the XRD patterns of CI and EI.

Sample	Phase	Space group	Weight fraction %	Cell parameters (Å)	Cell volume $(Å)^3$	FWHM (H_w) (2θ)	Crystallite size (nm)
CI	α-Fe	$Im\bar{3}m$ (bcc)	100	a=b=c=2.8615	23.43	0.931455 (44.753)	12
EI	α-Fe	$Im\bar{3}m$ (bcc)	100	a=b=c=2.8678	23.59	0.432666 (44.648)	25.8

4. Raman spectral parameters of FeC sample

Table S3. Raman absorption peak parameters of FeC sample.

Parameters	Sub-peaks					
	G	$D1_a$	$D1_b$	D2	D3	D4
Peak position	1588	1257	1346	1610	1494	1177
FWHM	82	57	144	32	180	111
Intensity	4354	890	9455	706	2875	2006

Table S4. Crystalline to disordered Raman peak intensity ratios for FeC sample.

Intensity ratio	I_G/I_D	I_G/I_{D2}	I_G/I_{D3}	I_G/I_{D1}	I_{G-D2}/I_{D1}	I_{G-D2}/I_D
Value	0.27	6.17	1.51	0.42	0.49	0.31

5. EDAX spectrum of FeC sample

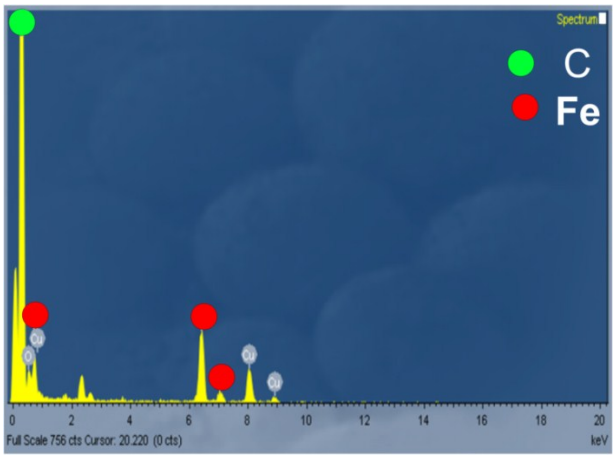

Figure S2. EDAX spectrum of FeC sample.

6. SE_A versus frequency for different thickness of PVDF-FeC specimens

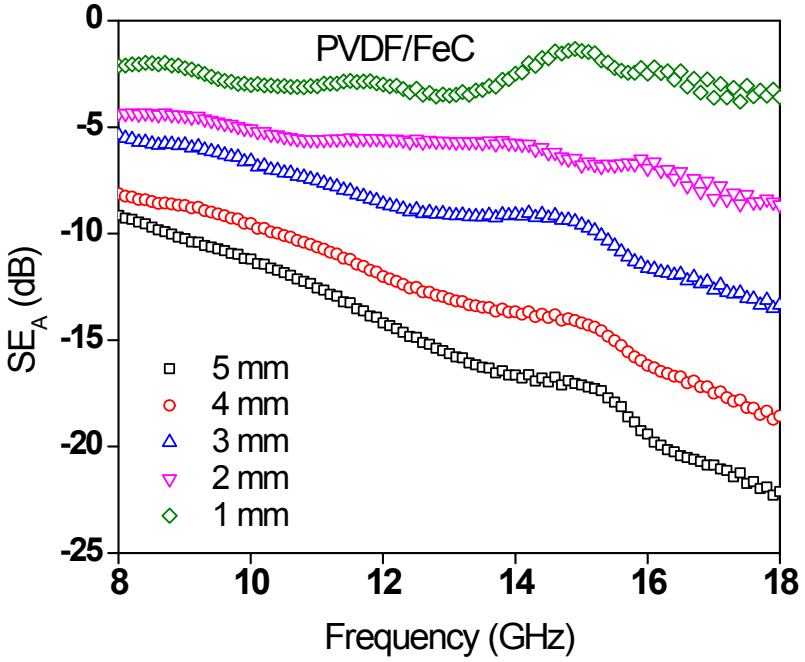

Figure S3. SE_A with respect to frequency at different thickness for PVDF/FeC specimen.

Fig. S3 shows the SE_A with respect to the frequency in the X and K_u band frequencies for PVDF/FeC specimen. It is seen that SE_A increases with thickness. For the 5 mm thick specimen the SE_A shows a value of - 26.6 dB at 18 GHz. The increase in SE_A with thickness indicates that shielding is mainly from absorption within the specimen and a minor contribution is due to reflection.

7. SE_T, SE_R and SE_A measured at 18 GHz for all the nanocomposites

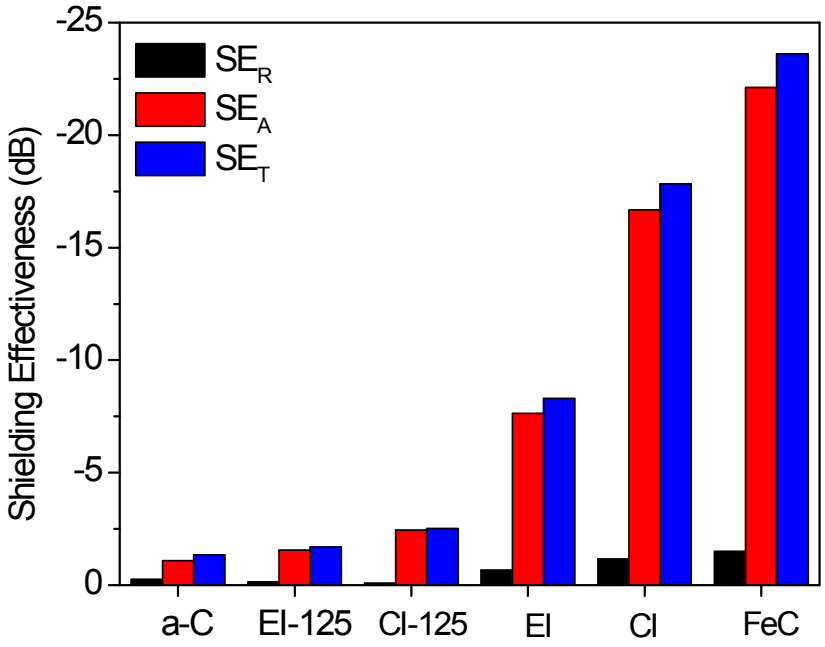

Figure S4. Comparison of SE_T, SE_R and SE_A measured at 18 GHz for all the nanocomposites.

Fig. S4 shows the comparison of SE_T, SE_A and SE_R at 18 GHz for all the nanocomposites, for 5 mm thick specimen. It can be observed that PVDF/FeC composite shows the maximum value of SE_T and SE_A which means the composite is very effective for microwave absorption. Compared to PVDF/a-C, the shielding in PVDF/FeC is increasing to a large extent. This implies that along with the magnetic particles, it is important to have a conducting layer of graphitic carbon which results in more EM absorption.

8. Complex permittivities and permeabilities of PVDF/CI, EI or a-C based composites

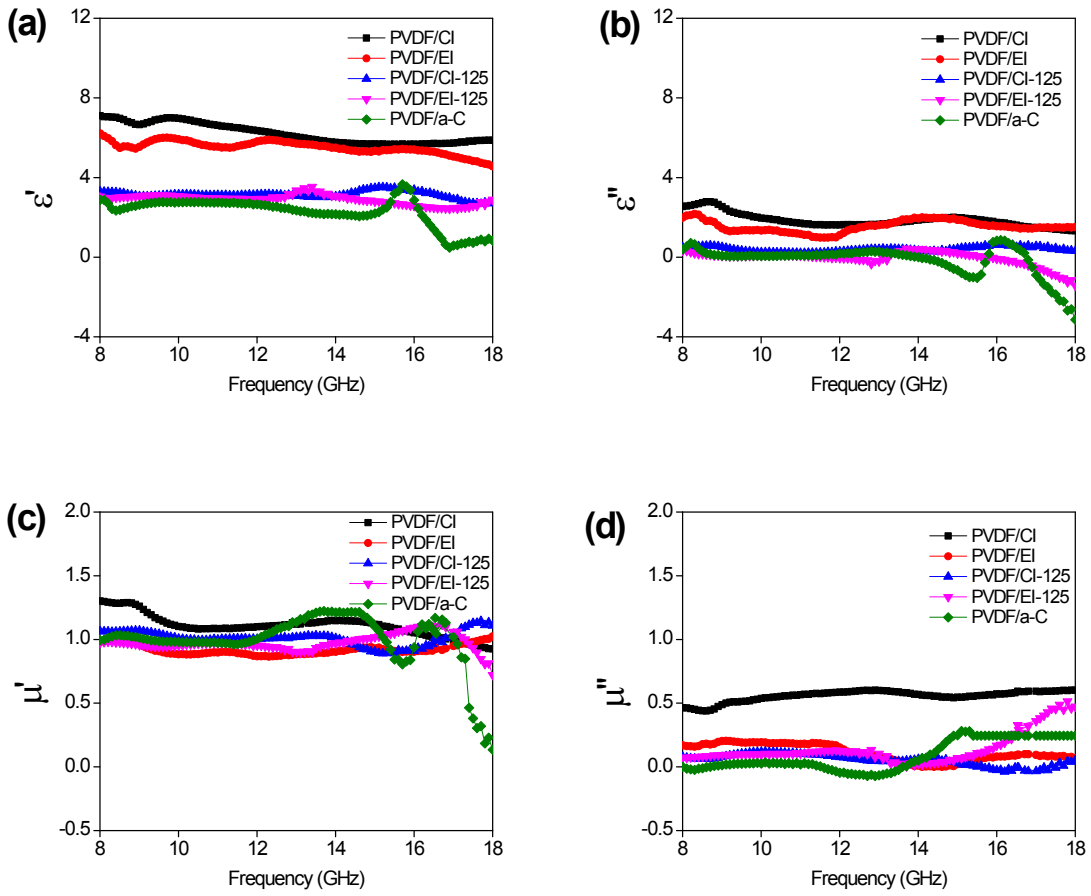

Figure S5. (a) Real part, (b) imaginary part of permittivity; (c) real part and (d) imaginary part of permeability in the frequency range of 8-18 GHz of (i) PVDF/CI, (ii) PVDF/EI, (iii) PVDF/CI-125, (iv) PVDF/EI-125 and (v) PVDF/a-C composite at 5 mm thickness.

Fig. S5 shows the complex permittivity and complex permeability of the nanocomposites in the X and K_u band frequencies. The dielectric constant and dielectric loss (ε′ and ε″) of PVDF/a-C, PVDF/CI-125 and PVDF/EI-125 composites is negligible. The PVDF/CI and PVDF/EI show higher values of ε' and ε''. Therefore the shielding in PVDF/CI and PVDF/EI is more than their less weight-fraction counterpart and also to PVDF/a-C. For the CI and EI containing samples the dielectric losses are mainly due to the interfacial polarization between iron and PVDF. The magnetic loss in all the samples is quite low at the microwave frequencies,

but in case of PVDF/CI shows higher value of μ'', which makes the PVDF/CI composite, magnetically lossy.

9. Cole-Cole plot of PVDF/FeC

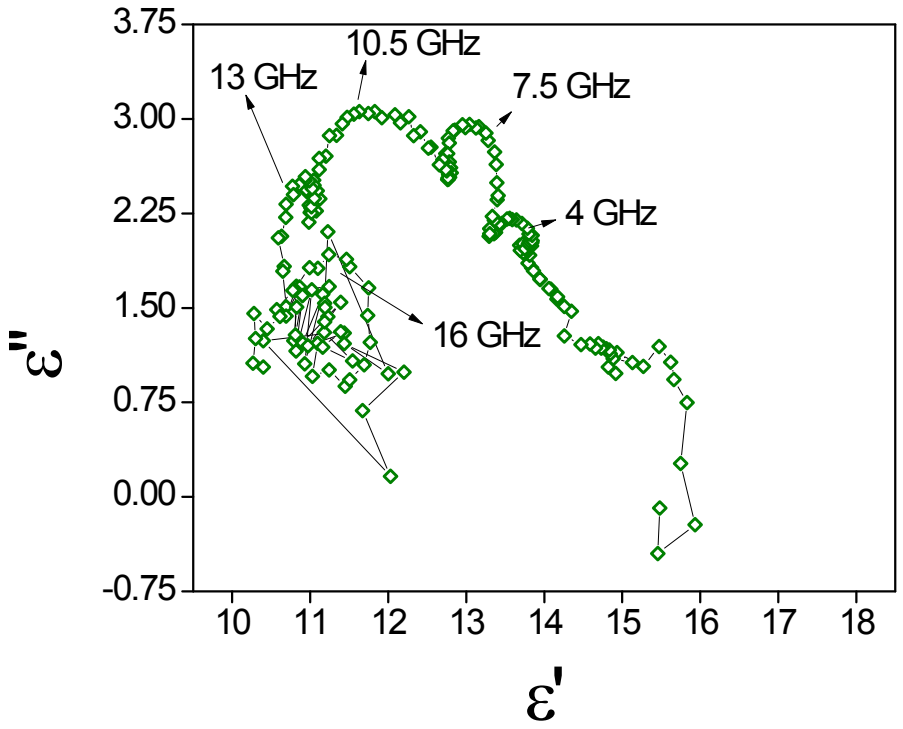

Figure S6. Cole-Cole plot of PVDF/FeC composite.

Fig. S6 shows the Cole-Cole plot of PVDF/FeC composite. The plot of ε' vs ε'' is called the Cole-Cole plot. For Debye type of relaxation, the Cole-Cole plot is a perfect semicircle. This semicircle represents the relaxation process in the sample. The multi-semicircles observed in Fig. S5 indicate that there are multiple dielectric relaxation processes, which are attributed to the size distribution of nanoscopic iron particles embedded in the graphitic carbon shells. The relaxation is the reason for the electromagnetic loss/absorption. This enhances the Maxwell-Wagner-Siller polarizations for PVDF/FeC composite [8].

10. Performance of the PVDF based composites

Table S1 compares the performance and weight of various PVDF based composites. We have explored in detail the possible mechanism for the synergistic effect of carbon encapsulation and dispersion of the embedded magnetic nanoparticles. A comparison has been made with composites prepared with only magnetic (iron) or only amorphous carbon components.

We see a lower SE_T than those reported in other literatures. But, in most of those cases the reflection component (SE_R) can be very high and such materials, although showing high SE_T, do not effectively reduce the EMI pollution. However, our synthesized sample proves that the same amount of metallic phases (CI or EI) lead to quite low SE_T in comparison to the specimen where the metallic phase is dispersed in carbon matrix (FeC). This indicates that using a similar amount of the metallic phase encapsulated in carbon matrix (similar to that of the FeC sample) may lead to much higher SE_T.

We have used co-axial wave guide technique for EMI shielding. In the references listed in Table S1, rectangular wave guide technique was used. Therefore, the direct comparison of the results cannot be made. Also, the present manuscript aims at identifying the role of synergistic interaction between carbon and magnetic particles. In this regard, our synthesized sample, which is a complex heterostructure, can prove to be an ideal candidate having both light-weight (amorphous) carbon and magnetic nanoparticles in close vicinity. We have tried to explain the role of individual component, i.e., magnetic particles and amorphous carbon by comparing with CI, EI and amorphous carbon. We concluded that it is indeed the synergistic interaction between the two components that leads to a higher EMI shielding. As we explained earlier, our focus was more to understand the mechanism of EMI shielding rather than enhancing the EMI shielding efficiency. However, the value of SE_T can be enhanced simply via the addition of a few (3-5) wt% of CNT or graphene in the composites. Although this is not the aim of the study, it will be verified in the future.

11. The RL plots of PVDF/CI and PVDF/EI composite

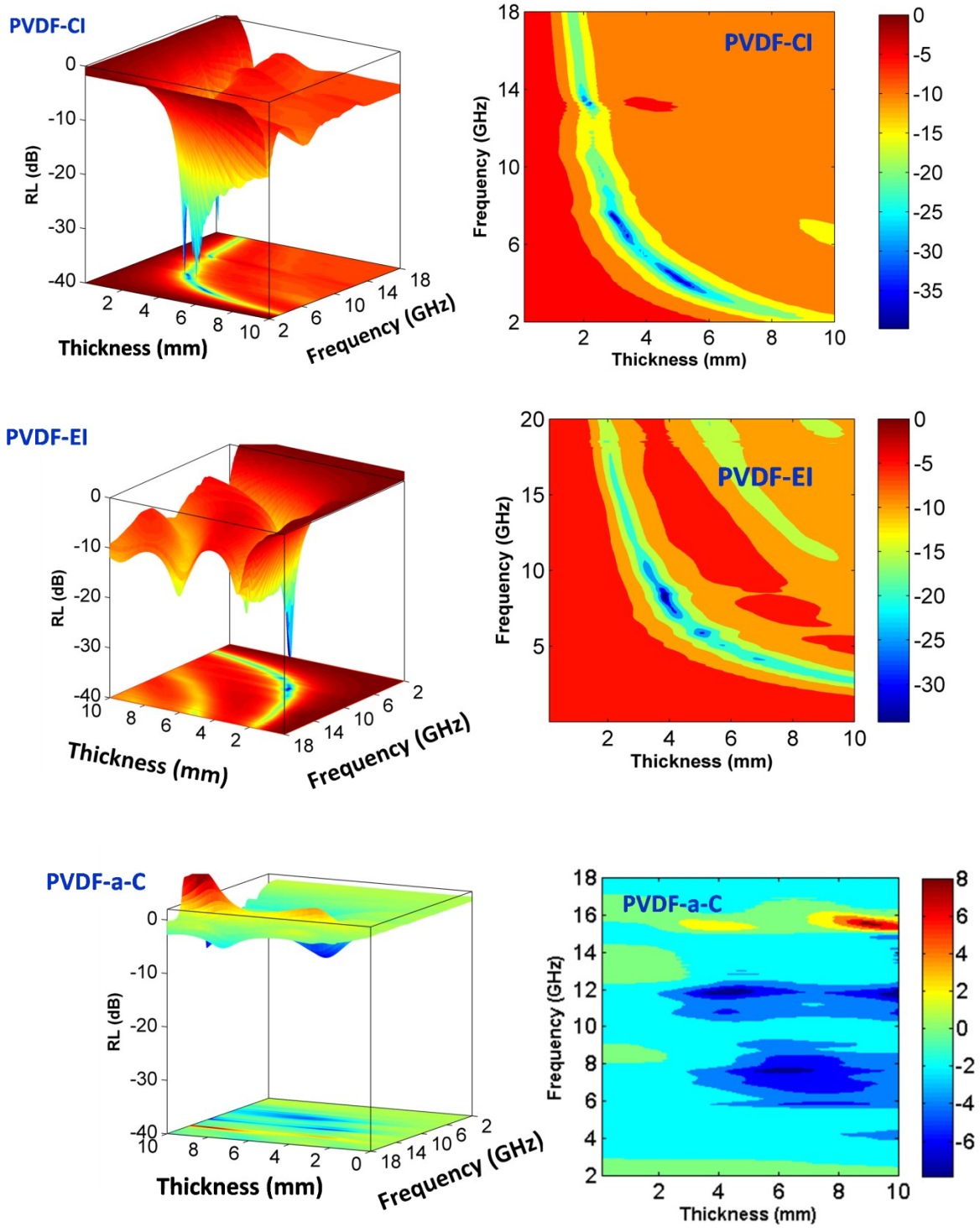

Figure S7. Calculated 3D-RL plot and contour map of nanocomposite with varying thickness and frequency.

The calculated 3D reflection loss plots of PVDF/CI, PVDF/EI, and PVDF/a-C are shown in Fig. S7. For PVDF/CI the RL has minimum value of - 42.6 dB. PVDF/EI shows the RL minimum at - 25 dB. PVDF/a-C composite shows very low value of RL minimum, indicating that amorphous carbon is least suitable of microwave absorption. Here one important thing to observe is that the CI particles have wider particle size distribution than EI. Thus, frequency range spread in the RL is more for PVDF/CI composites. Therefore, in this case the spherical shaped CI particles contribute towards enhanced RL than flaky EI particles [9-11].

References

[1] N. Joseph, J. Varghese, M.T. Sebastian, Graphite reinforced polyvinylidene fluoride composites an efficient and sustainable solution for electromagnetic pollution, Composites Part B: Engineering 123 (2017) 271-278

[2] J. Arranz-Andrés, E. Pérez, M. Cerrada, Hybrids based on poly (vinylidene fluoride) and Cu nanoparticles: Characterization and EMI shielding, European Polymer Journal 48(7) (2012) 1160-1168

[3] R. Dou, Y. Shao, S. Li, B. Yin, M. Yang, Structuring tri-continuous structure multiphase composites with ultralow conductive percolation threshold and excellent electromagnetic shielding effectiveness using simple melt mixing, Polymer 83 (2016) 34-39

[4] H. Gargama, A. Thakur, S. Chaturvedi, Polyvinylidene fluoride/nanocrystalline iron composite materials for EMI shielding and absorption applications, Journal of Alloys and Compounds 654 (2016) 209-215

[5] N. Joseph, S.K. Singh, R.K. Sirugudu, V.R.K. Murthy, S. Ananthakumar, M.T. Sebastian, Effect of silver incorporation into PVDF-barium titanate composites for EMI shielding applications, Materials Research Bulletin 48(4) (2013) 1681-1687

[6] N. Joseph, M.T. Sebastian, Electromagnetic interference shielding nature of PVDF-carbonyl iron composites, Materials Letters 90 (2013) 64-67

[7] H. Wang, K. Zheng, X. Zhang, X. Ding, Z. Zhang, C. Bao, L. Guo, L. Chen, X. Tian, 3D network porous polymeric composites with outstanding electromagnetic interference shielding, Composites Science and Technology 125 (2016) 22-29

[8] X. Jian, B. Wu, Y. Wei, S.X. Dou, X. Wang, W. He, N. Mahmood, Facile Synthesis of Fe3O4/GCs Composites and Their Enhanced Microwave Absorption Properties, ACS Applied Materials & Interfaces 8(9) (2016) 6101-6109,10.1021/acsami.6b00388.

[9] L.Z. Wu, J. Ding, H.B. Jiang, L.F. Chen, C.K. Ong, Particle size influence to the microwave properties of iron based magnetic particulate composites, Journal of Magnetism and Magnetic Materials 285(1–2) (2005) 233-239,http://dx.doi.org/10.1016/j.jmmm.2004.07.045.

[10] X. Wang, R. Gong, P. Li, L. Liu, W. Cheng, Effects of aspect ratio and particle size on the microwave properties of Fe–Cr–Si–Al alloy flakes, Materials Science and Engineering: A 466(1–2) (2007) 178-182,http://dx.doi.org/10.1016/j.msea.2007.02.051.

[11] V. Bhingardive, S. Suwas, S. Bose, New physical insights into the electromagnetic shielding efficiency in PVDF nanocomposites containing multiwall carbon nanotubes and magnetic nanoparticles, RSC Advances 5(97) (2015) 79463-79472,10.1039/C5RA13901E.